AIMS Materials Science, 12(1): 28–47.
DOI: 10.3934/matersci.2025003
Received: 27 October 2024
Revised: 26 December 2024
Accepted: 13 January 2025
Published: 20 January 2025

http://www.aimspress.com/journal/Materials

Research article

Microstructural evolution and direct shear strength of cement-stabilized soil under freeze-thaw cycles

Congyan Zhang[1,*], Feng Chen[2,*] and Xudong Wang[1]

[1] Yuanpei College, Shaoxing University, Shaoxing 312000, China
[2] Zhejiang Industry Polytechnic College, Shaoxing 312000, China

* **Correspondence:** congyanzhang@usx.edu.cn; chenfeng@zjgyzyjsxy.wecom.work; Tel: +86-178-5750-8575.

Abstract: Extensive research has demonstrated that cement is one of the most effective materials for improving soil properties. Researchers have investigated cement-stabilized soil techniques from various perspectives, including microstructural evolution and mechanical performance. However, studies on cement-stabilized soils in seasonal frozen regions remain limited. This study thus explored the application of cement-stabilized soil in these regions, specifically examining the effects of freeze-thaw cycles on its microstructure and shear strength through scanning electron microscopy (SEM) and direct shear tests. The findings indicate that freeze-thaw cycles induce noticeable microcracks and pores, significantly increasing particle breakage and decomposition, which leads to a loose structure and severely compromises the soil's mechanical properties. Incorporating cement generates hydration products that form cementitious bonds between soil particles, significantly enhancing structural density and overall stability. This cement stabilization effectively mitigates the damage caused by freeze-thaw cycles, enabling the soil to maintain good shear strength even after such cycles. These findings underscore the importance of cement stabilization in improving soil performance under freeze-thaw conditions, providing a theoretical basis and technical support for foundation improvement in cold regions.

Keywords: cement-stabilized soil; freeze-thaw durability; microstructure; direct shear strength; stabilized soil performance

1. Introduction

Limited land resources and increasing engineering activities require construction on problematic soils, making soil improvement a prevalent issue in engineering foundations. To improve the properties of these soils and enhance their stiffness and strength, extensive research has been conducted [1–5]. Stabilization techniques are considered to be one of the most effective methods to improve soil characteristics and make them suitable for civil engineering applications [6]. Researchers have employed various materials for soil modification, including sand, lime, fly ash, and volcanic ash [7]. Peethamparan et al. [8] analyzed the microstructural changes in cement kiln dust-reinforced sodium montmorillonite using X-ray diffraction (XRD), thermogravimetric analyzer (TGA), and scanning electron microscopy (SEM). Bahadori et al. [7] assessed the effects of different types of volcanic ash on the stability of marl soil and found that volcanic ash effectively enhances soil strength and durability, with stronger effects with higher content. They also investigated the influence of fly ash and volcanic ash on the stability of Umea Lake peat, showing that both can increase the unconfined compressive strength (UCS) of peat and improve bearing capacity, with the effects depending on organic matter and moisture content, stabilizer content, and particle size [9]. Additionally, Song et al. [10] studied the impact of basalt fibers on the mechanical properties of lateritic soil through direct shear tests and microstructural analysis, finding a significantly improved shear strength. In summary, the use of various materials and chemical binders for soil stabilization has become a common practice [11–13], with lime and cement being commonly used modifiers [14,15]. Unlike lime-based stabilizers that require appropriate temperature and pH conditions to be effective [14], cement-based stabilizers perform well across different soil types and curing conditions, making them one of the most widely used stabilization materials [16].

As early as 1966, Mitchell et al. [17] utilized electron microscopy to investigate particle changes during the hydration process of mixtures of silicate cement and natural silty clay. They found that in the initial stages of hydration, the cement hydration gel formed along the edges of the clay particles. As hydration progressed, the soil particles gradually disintegrated, and the hydration gel diffused throughout the soil matrix, ultimately forming an indistinguishable soil-cement composite. Lemaire et al. [14] examined the microstructure of lime- and cement-stabilized plastic silty soils using SEM and observed that after 28 days of treatment, the gel substance formed by cement covered the soil surface. Elemental distribution mapping and mercury intrusion porosimetry (MIP) analysis indicated that cement significantly improved the soil microstructure. XRD analysis monitored the physicochemical evolution, showing that the formation of hydration gels resulted in a “honeycomb” microstructure, significantly enhancing the soil’s mechanical properties. Islam et al. [18] stabilized tropical soft peat using cement and bentonite binders; through SEM and energy-dispersive X-ray (EDX) tests, they observed changes in the microstructure that markedly improved the peat’s bearing capacity. Horpibulsuk et al. [19] conducted qualitative and quantitative analyses of the microstructure of cement-reinforced silty clay during a 7-day curing period, finding that cement improved soil structure by increasing inter-particle bonding and reducing porosity. Du et al. [20] revealed through SEM the microstructural changes in cement-stabilized marine soft clay containing organic matter, showing that the formation of hydration products reduced porosity and made the soil microstructure denser, thereby increasing soil strength.

Numerous researchers have extensively studied fundamental mechanical properties, strength [21,22], and deformation patterns of cement-blended soil and cement mortar composite

soils [23–25], providing reliable engineering support [26]. Shihata et al. [27] identified the potential of using the UCS of cemented soil as a reliable durability indicator. Bouassida et al. [28], based on a three-dimensional scaling model of improved soft soil foundations, utilized the dynamic method of yield design theory to analyze the ultimate bearing capacity of soft-soil foundations improved via end-bearing soil-cement columns. Horpibulsuk et al. [29] further investigated the impact of cementation on clay behavior and summarized the mechanical properties of cemented clay, proposing new empirical formulas that consider the effects of cementation on strength and plastic deformation. Jongpradist et al. [30] found that the strength of cement-blended soil does not increase linearly with cement content and proposed using an effective void ratio to capture the mechanical properties of cement-clay additives under different test conditions, thereby quantifying the impact parameters in unconfined compressive tests. Wang et al. [31] studied the relationship between sand content and strength in cement mortar composite soil in the Hetao Irrigation District, finding that adding an appropriate amount of sand can effectively improve the structure and strength of cemented soil, with an optimal sand content leading to the highest strength and a distinct peak in the stress-strain curve. Farouk et al. [32] mixed two types of natural silt-sand soils from the Nile Delta with cement, preparing samples with different cement dosages and water/cement ratios, and studied their unconfined compressive strength. The results indicated that cement-improved soils showed significantly reduced settlement and increased compressive strength even at lower cement dosages. Gyeongo et al. [33] conducted shear and UCS tests on four types of marine dredged clay with varying water and cement contents, proposing two formulas for assessing early-stage strength. Chian et al. [34] performed a series of UCS tests on cement-stabilized soft clays with different sand particle contents, finding that the UCS of cement-stabilized samples decreased with increasing sand content. Du et al. [35] conducted loose undrained stress-controlled cyclic triaxial shear tests on cement and lime-stabilized organic matter-doped sand (OMDS) samples widely distributed in Hainan Province, China, under different confining pressures, curing periods, and cement contents. They obtained the maximum elastic modulus, normalized elastic modulus, and maximum dynamic damping ratio, systematically analyzing the effects of cement content, curing time, and initial confining pressure on these three parameters. Wahab et al. [36] stabilized fibrous, hemic, and sapric peat using different cement dosages, observed the stabilized strength through UCS tests, and verified morphological and chemical composition changes during stabilization using XRD and scanning electron microscopy energy dispersive spectrometer (SEM-EDS). The results showed that as cement products such as calcium silicate hydrate (CSH) formed, carbon significantly decreased, and calcium oxide increased. The strength of stabilized peat increased with cement dosage and curing time, demonstrating that cement as a binder can significantly enhance peat properties and identifying the optimal cement dosages for fibrous, hemic, and sapric peat.

Researchers have focused not only on the effects of cement-stabilized soil in natural environments but also on the stabilization effects of different additives under various conditions. Fatahi et al. [37] investigated the impact of polypropylene and recycled carpet fibers on the three-dimensional shrinkage behavior of cement-treated kaolinite and bentonite. They found that the combination of cement and fibers effectively reduced the volume changes of clay during drying, with cement having a more significant effect on reducing shrinkage in kaolinite, while fibers were more effective in bentonite. Du et al. [38] examined the engineering properties of zinc-contaminated kaolinite treated with cement additives, noting that zinc delays hydration and cementing reactions, significantly affecting the phase composition and microstructure of hydration products. Zhao et al. [39]

conducted cement modification tests on highly expansive soils in the Handan region of Hebei, finding that cation exchange capacity is not a valid indicator for assessing the expansion performance of cement-stabilized expansive soils. Liang et al. [40] studied the mechanical properties and microstructure of cement and fly ash-stabilized sludge through wet-dry cycle tests, revealing specific change patterns in these properties with varying cycle numbers and additive content. Zidan [41] conducted a comprehensive laboratory investigation on cement-stabilized cohesive soils, evaluating undrained shear strength and consolidation characteristics under different conditions. Phutthananon et al. [42] developed a novel state parameter for characterizing the mechanical properties of cement-treated clay. Du et al. [23] assessed the effect of organic matter on cement-stabilized marine soft clay through SEM and UCS tests, establishing a model relating strength to organic content. Ge [6] investigated the stabilization effects of organic matter and cement content on sludge, finding that electroosmosis treatment significantly improved the bearing capacity of organic sludge. Chandu et al. [43] enhanced the mechanical properties of cement-stabilized marginal laterite by adding foundry sand, maintaining strength after multiple wet-dry cycles. Xu et al. [44] simulated the meso-mechanical properties of cement-stabilized clay with low sand content using finite element methods. Liang et al. [45] studied the effects of sand content and particle size on the strength and durability of cement-consolidated marine soft clay in South China, finding improvements with increased sand content and decreased particle size. Joyce et al. [46] explored the impact of uncalcined limestone on cement-treated clay composites, discovering that both limestone and granite powder could be reused without significantly reducing unconfined compressive strength while reducing cement usage and providing environmental benefits. Phutthananon et al. [47] experimentally investigated the strength and microstructural characteristics of cement-bottom ash-mixed Bangkok clay, focusing on the efficiency of adding different concentrations of bottom ash (BA) as a cementing material. TGA and SEM analyses elucidated changes in microstructure and elemental composition/distribution, explaining the significant increase in the strength of cement-BA mixed clay.

In cold regions, freeze-thaw cycles exacerbate soil issues, thereby drawing significant attention to the study of soil and its modification in seasonally frozen soil areas. Chen et al. [48] found that regardless of the changes in dry density and salt concentration of clay samples, the permeability coefficient of compacted samples significantly increased after the first freeze-thaw cycle, indicating the necessity of modifying soils in cold regions. Yarba et al. [49] used mixtures of silica fume-lime, fly ash-lime, and red mud-cement as additives to stabilize two granular soils derived from primary rocks. Through freeze-thaw cycles, compressive strength, and ultrasonic testing, they investigated the effects of these additives on the freeze-thaw characteristics of soil samples, demonstrating that these mixtures can effectively improve the freeze-thaw durability of soils. Liu et al. [50] conducted dynamic triaxial tests and freeze-thaw cycle experiments on cement and lime-stabilized soils with different mixing ratios, studying threshold deviator stress and elastic modulus. The results indicated that the performance of stabilized soils significantly improved after multiple freeze-thaw cycles, with cement-stabilized soil outperforming lime-stabilized soil. Miraki [16] used environmentally friendly binders with lower carbon footprints, such as alkali-activated ground granulated blast-furnace slag (GGBS) and volcanic ash (VA), to stabilize soils. Mechanical and microstructural tests showed that the combination of GGBS and VA more effectively enhanced soil's resistance to wet-dry and freeze-thaw cycles. Sagidullina et al. [51] employed calcium sulfoaluminate (CSA) cement, which has a lower carbon footprint, for soil treatment. UCS and ultrasonic pulse velocity (UPV) tests revealed

that with an increase in freeze-thaw cycles, the strength and pulse velocity values declined, but soil performance improved with higher cement content, proving that CSA can achieve sufficient base strength as a stabilizer for silty sand. Ma et al. [52] studied the dynamic strength properties (strength parameters and dynamic critical stress) of silty clay before and after cement improvement under different confining pressures through dynamic triaxial tests. They confirmed that the dynamic strength of cement-stabilized clay (CSC) was effectively enhanced and maintained high dynamic strength even after multiple freeze-thaw cycles.

In summary, cement-stabilized soils, as an important engineering material, have been extensively applied and studied in various fields. Researchers have delved into its fundamental properties, preparation methods, processes, and engineering applications, yielding significant findings. However, several deficiencies and issues requiring further investigation remain. For instance, in experimental design, the influence of different admixture ratios and curing times necessitates optimization to enhance the reliability and repeatability of results. Particularly, substantial work is needed to study the shear properties of cement-stabilized soils under freeze-thaw cycles. This paper employs SEM and direct shear tests to visually analyze the microstructural evolution of cement-stabilized soils and investigates the changes in direct shear strength under freeze-thaw cycles, providing a reference for foundation modification in cold regions.

2. Materials and methods

2.1. Experimental materials

The cement used was P.O. 42.5, supplied by Yisen Technology Co. The soil was dried, crushed, ground, and sieved to particles smaller than 0.3 mm, then oven-dried at 105 °C for future use. The main chemical composition, shown in Table 1, was determined using X-ray fluorescence (XRF) analysis.

Table 1. Major chemical composition of the soil used in the experiments.

Clay composition	MgO	Al_2O_3	SiO_2	K_2O	FeO	Na_2O	Others
Clay content (wt%)	1.11	25.17	66.11	2.63	3.60	1.22	0.15

2.2. Sample preparation

The oven-dried soil particles were mixed with Portland cement at specified ratios to ensure a uniform and consistent powder mixture. The water-to-powder mass ratio (w/p), referring to this mixture, and the cement-to-soil mass ratios (c/s) based on experimental conditions are shown in Tables 2–4. Untreated soil samples and pure cement samples were prepared as control groups. Each mix proportion had three groups with three samples each, totaling nine samples per proportion.

Table 2. Mix proportion used in XRD analysis.

w/p for XRD	c/s for XRD	Designated ages
0.5	1:5	3, 14, and 28 days
	2:1	
	Untreated soil	
	Pure cement	

Table 3. Mix proportion used in SEM analysis.

w/p for SEM	c/s for SEM	Designated ages
0.5	1:5	3, 14, and 28 days
	1:2.5	
	1:1	
	Untreated soil	

Table 4. Mix proportion used in direct shear testing.

w/p for direct shear testing	c/s for direct shear testing	Designated ages
0.4 and 0.5	1:5	28 days
	1:2.5	
	1:1	
	Untreated soil	

2.3. Preparation of cement-stabilized soil microstructure samples

The thoroughly mixed experimental materials with different w/p and c/s ratios were poured into clean, dry molds to form cubic specimens measuring 40 × 40 × 40 mm (Figure 1a). These specimens were initially cured in a standard curing chamber at 20 ± 2 °C and 95% humidity. After 24 h of curing, specimens were demolded. To ensure complete cement hydration, specimens continued to be cured under the same conditions until the designated ages of 3, 14, and 28 days (Figure 1b).

After curing, specimens were crushed, and the central portions were immersed in alcohol to terminate the hydration process; they were then dried in a vacuum desiccator. Appropriately sized samples were selected for SEM analysis (Figure 2a). Selected samples were coated with a thin layer of gold to enhance their conductivity. SEM examination was conducted at a working distance of 10 mm and an accelerating voltage of 15 kV, allowing for high-resolution imaging of the microstructural features.

The remaining portions were ground into powder (Figure 2b) for XRD analysis to determine the compositional phases. The grinding process involved breaking down the larger fragments using a mortar and pestle, followed by mechanical grinding to achieve a uniform powder. The powder was then sieved to obtain fine and consistent particles, ensuring precise XRD measurements. The prepared powder was packed into the sample holder with a flat and even surface. XRD analysis was conducted with the tube voltage set to 45 kV and the tube current set to 40 mA, allowing accurate identification of crystalline phases.

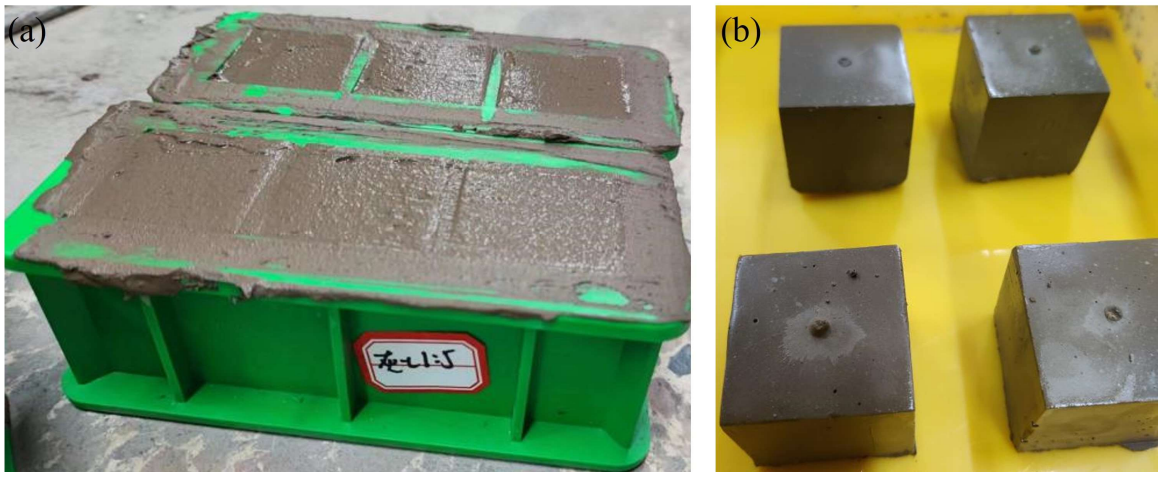

Figure 1. Cast specimens. (a) Samples in molds; (b) demolded samples.

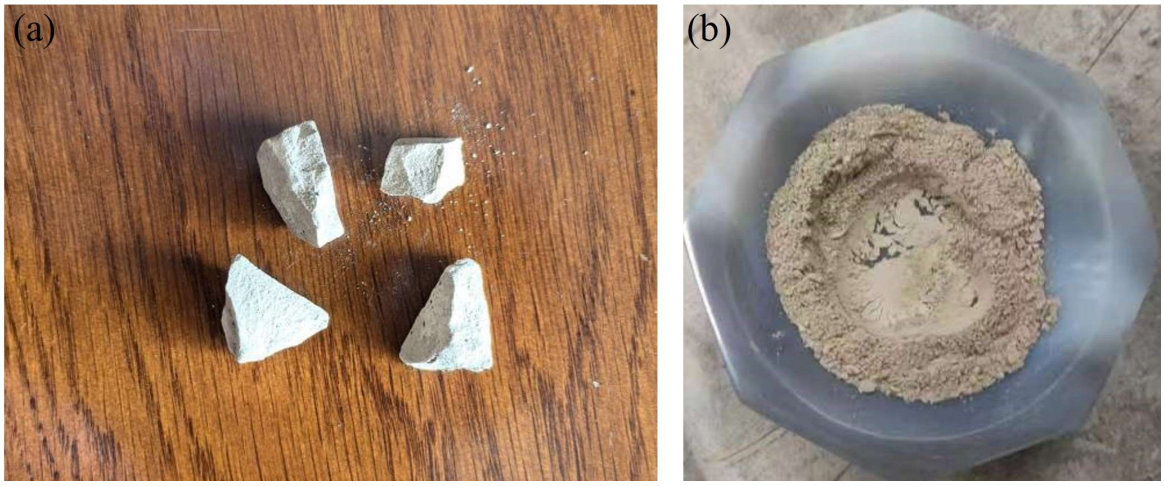

Figure 2. Experimental samples for analysis. (a) SEM samples; (b) XRD samples.

2.4. Preparation of samples for shear performance testing of cement-stabilized soil

The thoroughly mixed experimental materials with different w/p and c/s ratios were poured into cleaned and dried molds to form cylindrical specimens with 100 mm diameter and 200 mm height (Figure 3a). These specimens underwent initial curing in a standard curing chamber at 20 ± 2 °C and 95% humidity. After 24 h, specimens were demolded. To ensure complete cement hydration, demolded specimens were divided into two batches for further curing until the specified ages. The first batch was subjected to direct shear testing after 28 days of curing, with the loading rate controlled at 0.05 mm/min. The second batch, after 24 days of curing, was immersed in water at 20 °C and cured for 28 days; then, it was removed, surface-dried, and placed in a freeze-thaw cycling chamber (Figure 3b). Freeze-thaw temperature ranged between −17 ± 2 and 8 ± 2 °C, with each cycle lasting 4 h. After 50 freeze-thaw cycles, specimens were subjected to direct shear testing, also with the loading rate controlled at 0.05 mm/min. The freeze-thaw cycling chamber used for the tests is shown in Figure 4.

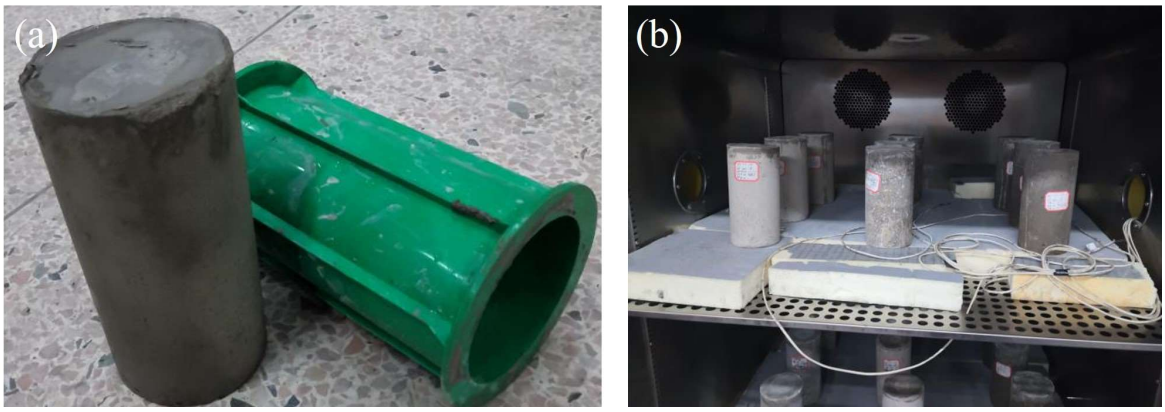

Figure 3. Samples for direct shear testing. (a) Demolded specimens; (b) specimens in the freeze-thaw cycling chamber.

Figure 4. Freeze-thaw cycling apparatus.

3. Results and discussion

3.1. XRD analysis

Figure 5a depicts the XRD results of the soil samples. The primary minerals identified in the soil include quartz, illite, and kaolinite, along with secondary minerals such as anorthite and phlogopite. Figure 5b shows the XRD results of pure cement with a water-to-powder (w/p) ratio of 0.5 at different hydration times (3, 14, and 28 days). At 3 days of curing (red), clinker minerals such as tricalcium silicate (C_3S) and dicalcium silicate (C_2S) remain largely unreacted, displaying prominent characteristic peaks. Early hydration products like calcium hydroxide ($Ca(OH)_2$, also known as CH) and ettringite begin to appear, albeit with low peak intensity. By 14 days of

curing (blue), more calcium silicate hydrates (C-S-H) are formed, increasing the hydration degree of C_3S and C_2S, which leads to a reduction in their peak intensities, while the peaks of CH and ettringite intensify. At 28 days (yellow), most C_3S and C_2S have hydrated, resulting in the formation of significant amounts of C-S-H gel and CH, with further reduction of unreacted clinker peaks and highly prominent CH peaks. These changes reflect the ongoing hydration reaction of cement over time, resulting in the formation of different products and altering the material's mineral composition and crystalline structure.

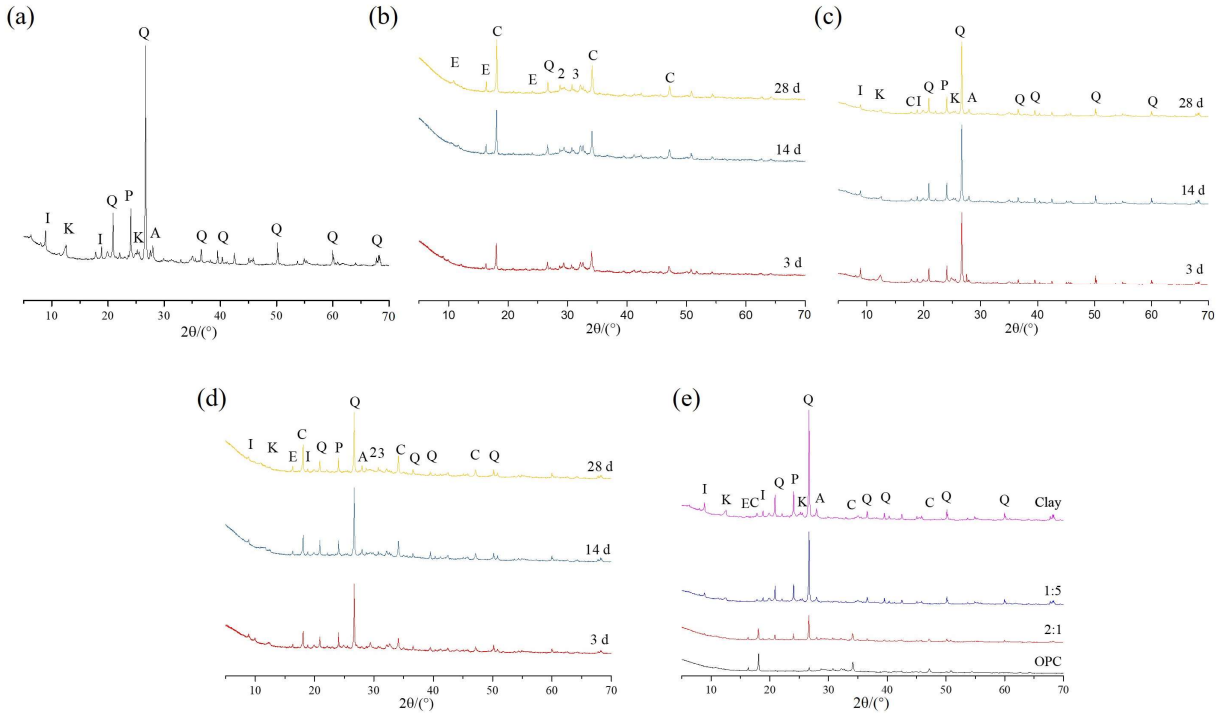

Figure 5. XRD results of experimental samples. (a) XRD pattern of untreated soil samples; (b) XRD patterns of cement at different hydration times: 3, 14, and 28 days; (c) XRD patterns of soil-cement mixture with a cement-to-soil ratio of 1:5 at hydration times of 3, 14, and 28 days; (d) XRD patterns of soil-cement mixture with a cement-to-soil ratio of 2:1 at hydration times of 3, 14, and 28 days; (e) comparative XRD patterns of samples with varying cement contents. 2: dicalcium silicate (C_2S); 3: tricalcium silicate (C_3S); A: anorthite; C: portlandite; E: ettringite; I: illite; K: kaolinite; P: phlogopite; Q: quartz.

Figure 5c illustrates the XRD results for soil samples mixed with cement (cement-to-soil (c/s) of 1:5) at different hydration times (3, 14, and 28 days). At 3 days (red), the primary cement minerals C_3S and C_2S begin to react, forming ettringite and some CH, while the original soil minerals (e.g., quartz, feldspar) remain predominant. By 14 days (blue), more C-S-H gel and CH are produced, reducing the intensity of the original cement clinker peaks. This indicates an increased conversion of cement minerals into hydration products. By 28 days (yellow), most of the cement has hydrated. This results in substantial amounts of C-S-H and CH, with very prominent CH peaks.

Figure 5d refers to the situation when the c/s is adjusted to 2:1, demonstrating more pronounced characteristic peaks of cement clinker minerals and hydration products (ettringite and CH), while the original mineral peaks diminish but remain significant. By 28 days, the majority of the cement has hydrated, forming extensive C-S-H and CH, making hydration products the dominant mineral phase in the mixture.

Figure 5e synthesizes the XRD results of the impact of varying cement content on soil. The primary minerals in untreated soil samples include quartz and illite. At a c/s ratio of 1:5 (blue), the peaks of cement and soil minerals overlap, with soil minerals still being predominant. Initial characteristic peaks of cement hydration products, such as CH, can be observed. At a c/s ratio of 2:1 (red), hydration products dominate the spectrum, with significantly enhanced peaks of CH and ettringite and diminished peaks of soil minerals. In pure cement (black) after 28 days, almost all the cement has converted into CH, ettringite, and C-S-H gel.

The XRD results for different w/p and c/s ratios at various curing stages illustrate the mineral phase evolution of cement and soil mixtures over time. This is critical for quality control and performance evaluation of cement-stabilized soils in practical engineering applications.

3.2. Microstructure

Figure 6 presents the SEM images of soil samples under different conditions. Figure 6a shows the SEM image of the original soil sample. The image reveals relatively large and intact soil particles. Despite the rough surface texture, there are no significant cracks or pores, indicating a compact overall structure with closely bonded particles and relatively low porosity.

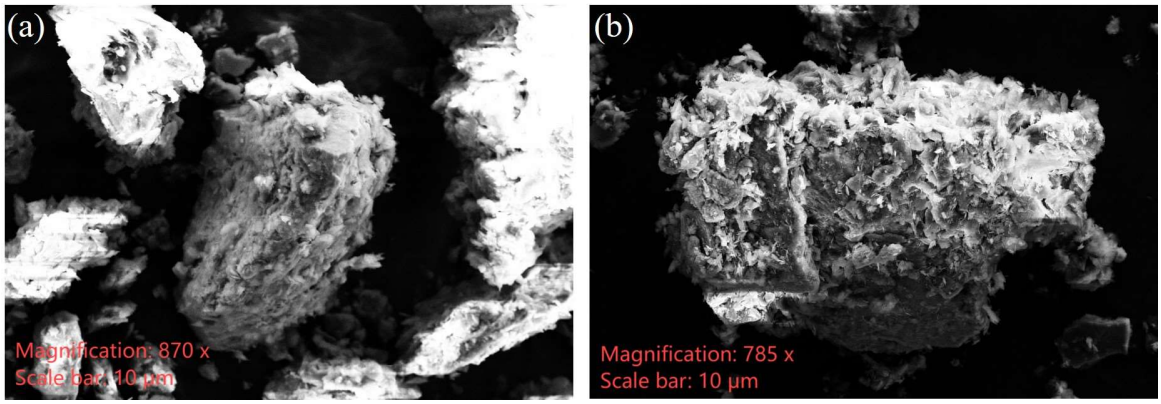

Figure 6. SEM results of the original soil samples under different conditions. (a) Original soil sample; (b) original soil sample after freeze-thaw cycles.

Figure 6b illustrates the SEM image of the soil sample after freeze-thaw cycles. The image shows an increase in fine particles and fragments, suggesting that the freeze-thaw processes have induced particle breakage and decomposition. Noticeable cracks and pores are evident, likely resulting from the volumetric expansion of water upon freezing. This expansion creates microcracks that further propagate during thawing, leading to particle disintegration. These cycles weaken particle bonding forces, with some particles appearing free. This phenomenon can be attributed to the continuous expansion and contraction of water during the freeze-thaw process, which disrupts the

binding materials between particles, resulting in a looser structure. Consequently, the porosity of the soil increases significantly, exhibiting loose and porous characteristics. These microstructural changes are expected to considerably influence the soil's mechanical, thermal, and hydrological properties, such as increasing permeability and decreasing load-bearing capacity.

Figure 7 illustrates the SEM images of samples with a c/s ratio of 1:5 under varying curing conditions. Figure 7a represents the sample cured for 14 days. Figure 7b shows the sample cured for 28 days. Figure 7c depicts the sample after 28 days of curing followed by freeze-thaw cycles.

Figure 7a shows that after 14 days of curing, cement particles have bonded with soil particles, forming a new structure. The surface of the particles exhibits gel-like substances encircling the soil particles. The distribution of crystalline and gel-like substances indicates that the cement has undergone hydration reactions, producing hydration products such as ettringite. These products act as a binder between particles, enhancing the overall compactness of the structure. However, the distribution of hydration products is relatively uneven, and voids between particles are not fully filled, resulting in numerous pores and some microcracks. Consequently, the overall structure remains relatively loose compared to untreated soil samples but more compact.

Figure 7b demonstrates that after 28 days of curing, the hydration reactions are more complete, resulting in the abundant formation of hydration products like ettringite. In some regions, large crystalline aggregates are observed. These hydration products effectively fill the voids between particles, significantly enhancing the binding effect. The interfacial transition zones become denser, and the bonding between cement and soil particles is more robust. Porosity is markedly reduced, microcracks are minimized, and the material's compactness and overall strength are significantly improved.

Figure 7c reveals that after freeze-thaw cycles, the internal porosity of the material increases significantly, and the structure is compromised. Microcracks proliferate. Noticeable cracks appear at the interfaces, weakening the overall strength of the material. The surfaces of soil and cement particles become rough, with some particles fracturing, indicating the damaging effects of freeze-thaw cycles on particle morphology. The hydration products may detach or disintegrate due to the freeze-thaw process, leading to a weakened binding structure.

By comparing Figure 7a,b, it is clear that the 14-day cured sample contains numerous unfilled voids and cracks, with a relatively loose structure and fewer hydration products in the interfacial zones, resulting in inadequate particle bonding. In contrast, after 28 days of curing, the hydration reactions are nearly complete, and the hydration products significantly fill the voids, markedly improving the compactness and strength of the structure. The interfacial zones exhibit stronger bonding, and the overall structural stability is significantly enhanced. This indicates that extending the curing time effectively improves the compactness and structural stability of the composite material.

Comparing Figure 7b,c, the sample without freeze-thaw cycles shows a dense and uniform microstructure. There is good bonding between the cement and soil particles, lower porosity, and abundant hydration products, all of which enhance its mechanical properties. After freeze-thaw cycles, the structure becomes noticeably loose. Porosity increases, bonding weakens, particle surfaces fracture, and microcracks expand. These changes make the material more brittle and significantly damage the microstructure.

In summary, extending the curing time significantly improves the microstructure and macroscopic mechanical properties of cement-soil composite materials. However, freeze-thaw cycles degrade their structure, reducing material strength and stability.

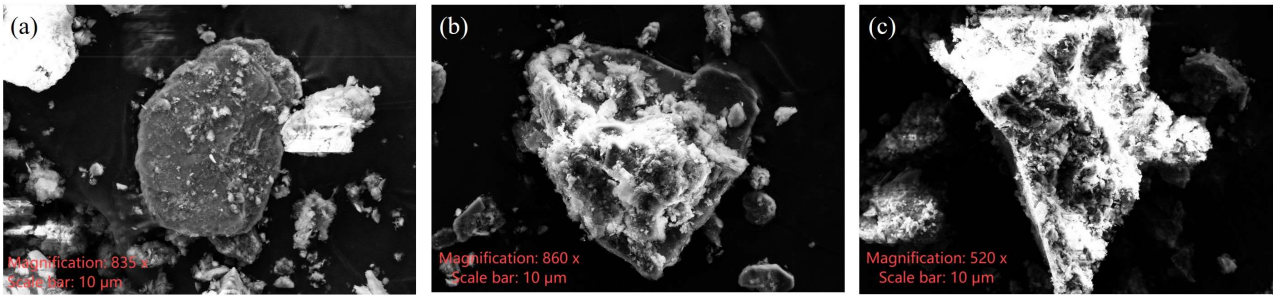

Figure 7. SEM results of samples with a cement-to-soil mass ratio of 1:5. (a) Cured for 14 days; (b) cured for 28 days; (c) cured for 28 days followed by freeze-thaw cycles.

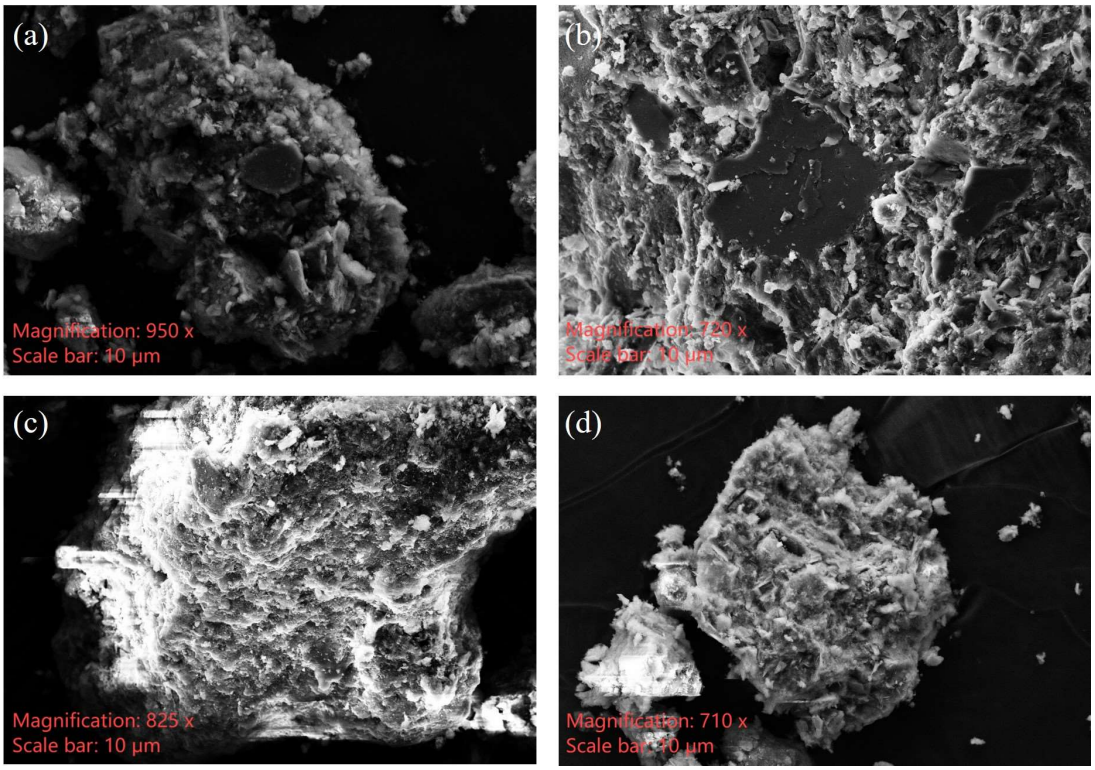

Figure 8. SEM results of samples with cement-to-soil mass ratios of 1:2.5 and 1:1 after 14 and 28 days of curing. (a) Sample with a cement-to-soil mass ratio of 1:2.5 and cured for 14 days; (b) sample with a cement-to-soil mass ratio of 1:1 and cured for 14 days; (c) sample with a cement-to-soil mass ratio of 1:2.5 and cured for 28 days; (d) sample with a cement-to-soil mass ratio of 1:1 and cured for 28 days.

Figure 8 presents the SEM images of samples with cement-to-soil mass ratios of 1:2.5 and 1:1 after 14 and 28 days of curing. By comparing Figure 8a,c and Figure 8b,d, the following observations can be made: after 14 days of curing, the hydration process is incomplete. Fewer hydration products are present on the surface, resulting in insufficient density and cohesion, weaker interfacial bonding, and higher porosity with larger pores. There are also relatively more cracks in both number and size. In contrast, after 28 days of curing, the degree of hydration is significantly enhanced. Hydration

products are more uniformly distributed and tightly bound. The interfacial bonding strength between particles is markedly improved, leading to a noticeable reduction in pores and cracks, and a significant increase in overall density.

Further comparison of Figure 8 with Figure 7 reveals the following: when the mass ratio is 1:1, the proportion of hydration products is highest. This effectively fills the inter-particle voids, resulting in the lowest porosity, fewest cracks, and highest structural density. Conversely, at a mass ratio of 1:5, the hydration products are minimal. This leads to poor bonding and the loosest structure, with prominent microcracks and the highest porosity. At a mass ratio of 1:2.5, a relatively high amount of hydration products enhances the bonding. However, porosity is slightly higher, and occasional microcracks are observed compared to the 1:1 ratio samples, with an overall slightly lower density. The porosity, number, and size of cracks are all less than those of the 1:5 ratio samples, and the interfacial bonding is stronger.

Figure 9 presents the SEM images of samples with a cement-to-soil mass ratio of 1:2.5 and 1:1 after 28 days of curing followed by freeze-thaw cycles. Results indicate significant microstructural damage, including increased porosity, more cracks, and loosening of particle interfaces. The originally dense structure becomes loose, surface roughness increases, and interfacial bonding between particles is severely compromised. Numerous interfacial cracks appear and, in some regions, there are fragmented hydration products and detached soil particles, leading to a marked decline in the overall stability of the microstructure.

Comparing Figure 9a,b, both ratios exhibit cracking and delamination of hydration products after freeze-thaw cycles. However, the sample with a higher cement content (1:1) still shows a relatively dense and uniform microstructure, with evenly distributed hydration products, less damage, stronger interfacial bonding, and limited expansion of pores and cracks. In contrast, the sample with a 1:2.5 ratio, having a higher soil content, exhibits more severe fracturing of hydration products and greater structural damage after freeze-thaw cycles. The comparison between Figures 9 and 7c further highlights this difference, indicating that a higher cement content enhances the material's freeze-thaw resistance.

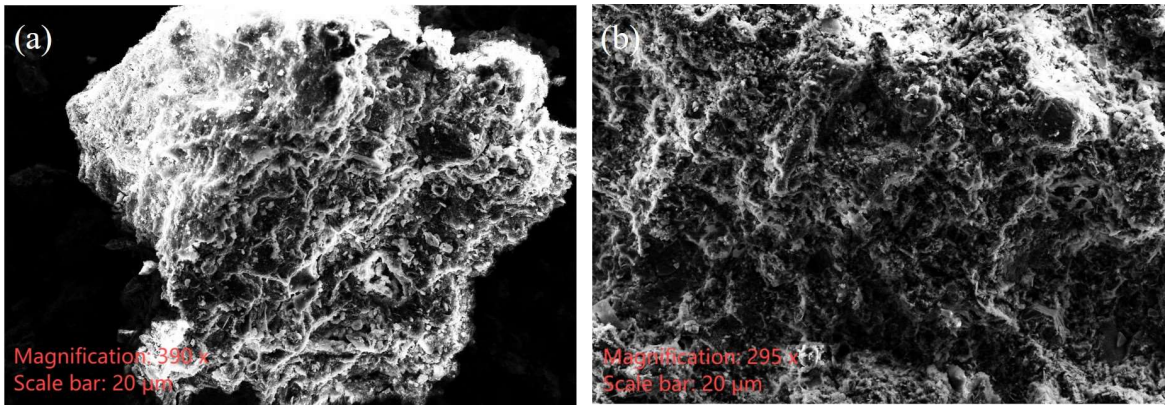

Figure 9. SEM results of samples with cement-to-soil mass ratios of 1:2.5 and 1:1 after 28 days of curing followed by freeze-thaw cycles. (a) Cement-to-soil mass ratio of 1:2.5; (b) cement-to-soil mass ratio of 1:1.

In this study, consistent with the findings of Chen et al. [48], we observed that freeze-thaw cycles have a destructive impact on the microstructure of soil, leading to the loss of its continuity and bearing capacity. Our experiments, conducted over 50 freeze-thaw cycles, confirmed that incorporating cement into the soil can effectively counteract the effects of freeze-thaw cycles. Notably, we found that within a certain range of cement content, the soil's resistance to freeze-thaw damage increased with higher cement content.

3.3. Shear performance of cement-stabilized soil

The direct shear tests and freeze-thaw direct shear tests were conducted on samples with different w/p and c/s ratios using a direct shear apparatus (Figure 10). Notably, the integrity of the untreated soil samples was severely compromised after multiple freeze-thaw cycles. This made it impossible to measure their direct shear strength, as depicted in Figure 11. The direct shear test results for other c/s ratios post freeze-thaw cycles are illustrated in Figure 12. In this figure, 0.4 and 0.5 represent the w/p ratios, and F indicates samples subjected to freeze-thaw cycles. The error bars in Figure 12 represent the standard deviation of multiple measurements, providing an indication of the variability of the data and, hence, the reliability of the results.

Figure 10. Direct shear apparatus.

The results demonstrate that, for the same w/p ratio, the direct shear strength of samples with a c/s of 1:5 is significantly lower than that of samples with a ratio of 1:2.5. The strength of the 1:5 samples is approximately 58% of the 1:2.5 samples when not subjected to freeze-thaw cycles. For a w/p ratio of 0.4, after freeze-thaw cycles, the direct shear strengths of the 1:5 and 1:2.5 samples decreased by 35.1% and 42.4%, respectively. The strength of the 1:5 sample is approximately 65% of the 1:2.5 sample. For a w/p ratio of 0.5, the reductions were 21.7% and 38.6%, respectively, with the 1:5 sample's strength being approximately 74.2% of the 1:2.5 sample.

Under the same c/s ratio, the direct shear strength of samples with a w/p ratio of 0.5 was approximately 68% of those with a ratio of 0.4. After freeze-thaw cycles, for samples with c/s ratios of 1:5 and 1:2.5, the direct shear strengths of those with a w/p ratio of 0.5 were 18.9% and 27.8% lower than those with a ratio of 0.4, respectively.

These findings indicate that cement content and w/p ratios significantly impact the direct shear strength of cement-soil composites. Higher cement content and lower w/p ratios result in higher direct shear strength. This effect remains substantial under freeze-thaw conditions. These results are

consistent with those of Ma et al. [52], indicating that the incorporation of cement and its increased content effectively enhance the strength of cement-stabilized soil. However, after 50 freeze-thaw cycles, we observed that this strength enhancement did not maintain the stabilized soil's strength; instead, it gradually decreased, potentially leading to a loss of load-bearing capacity. Notably, as the cement content increased, the rate of strength reduction slowed within a certain range. These findings provide important insights for the application of cement-soil composites under extreme climatic conditions.

Figure 11. Untreated soil samples after freeze-thaw cycles.

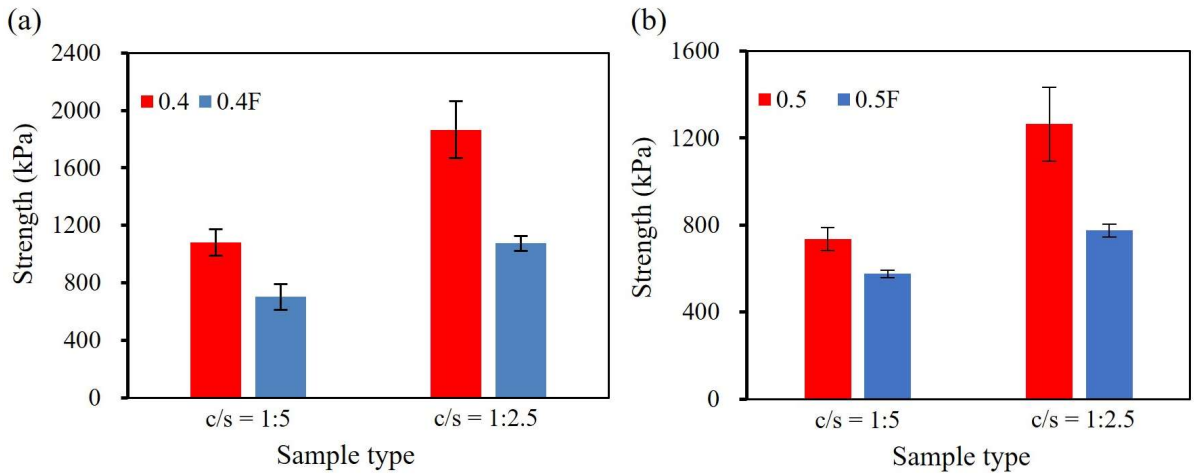

Figure 12. Direct shear test results for samples with different c/s and w/p ratios. (a) w/p = 0.4; (b) w/p = 0.5.

4. Conclusions

This study systematically investigated the impact of varying the cement-to-soil (c/s) and water-to-powder (w/p) ratios on the hydration process and structural properties of cement-soil

composites. The following advanced analytical techniques were employed: XRD was employed to track changes in mineral composition and hydration products. SEM was used to observe microstructural transformations pre- and post-freeze-thaw cycles. Direct shear tests were conducted to assess variations in shear strength before and after freeze-thaw cycles.

The key findings from this study are:

1. Soil composition and structure: the primary minerals in the soil, specifically quartz, illite, and kaolinite, contribute to a relatively loose soil structure, affecting its physical and chemical properties.

2. Cement hydration and structural enhancement: the incorporation of cement introduces clinker minerals such as tricalcium silicate and dicalcium silicate. As hydration progresses, hydration products like C-S-H gel and calcium hydroxide form, acting as binding agents between soil particles. This significantly enhances the density and overall stability of the structure. Under certain conditions, with increased cement content and decreased water-to-powder ratios, the binding effect becomes more pronounced, resulting in higher direct shear strength of the cement-soil composites.

3. Effects of freeze-thaw cycles: freeze-thaw cycles cause substantial disruption to the continuity of the soil structure, leading to significant microcracks, increased porosity, and particle fragmentation. This degrades the mechanical properties, rendering the soil structure loose and porous.

4. Practical applications: adding an appropriate amount of cement to the soil can effectively mitigate the structural damage caused by freeze-thaw cycles. This helps preserve structural integrity and ensures that the cement-soil composites retain favorable shear resistance after such cycles. These findings provide valuable insights into soil stabilization measures in cold regions, facilitating further exploration and optimization of related techniques.

In summary, these findings demonstrate the significant benefits of cement stabilization in enhancing soil performance under freeze-thaw conditions. Optimizing both cement and water content is essential for improving the stability and mechanical strength of cement-soil composites. Although this study explored specific soil types, its findings lay the foundation for future research. Future studies could explore cement alternatives and the application of cement (or cement alternatives)-stabilized soils under varying environmental conditions. Additionally, research could focus on the role of cement (or cement alternatives)-stabilized soils in the immobilization of contaminants (such as heavy metals). These efforts aim to further enhance the performance and sustainability of construction materials.

Use of AI tools declaration

The authors declare they have not used Artificial Intelligence (AI) tools in the creation of this article.

Acknowledgments

The authors are grateful for the financial support from the Joint Funds of the Zhejiang Provincial Natural Science Foundation of China, grant number LHY22E080001.

Author contributions

Conceptualization: C.Z.; methodology: C.Z.; validation: C.Z. and F.C.; formal analysis: X.W.; investigation: X.W.; resources: C.Z.; data curation: C.Z.; writing-original draft preparation: C.Z. and F.C.; writing-review and editing: C.Z. and F.C.; visualization: F.C.; supervision: F.C. and X.W.;

project administration: C.Z.; funding acquisition: C.Z. All authors have read and agreed to the published version of the manuscript.

Conflict of interest

The authors declare no conflicts of interest.

References

1. Carter JP, Liu MD (2005) Review of the structured cam clay model, In: Jerry A. Yamamuro PE, Victor NK, *Soil Constitutive Models: Evaluation, Selection, and Calibration*, Reston: American Society of Civil Engineers Publishing, 99–132. https://doi.org/10.1061/40771(169)5
2. Guo Y, Yu X (2016) Characterizing the surface charge of clay minerals with Atomic Force Microscope (AFM). *AIMS Mater Sci* 4: 582–593. https://doi.org/10.3934/matersci.2017.3.582
3. Lyu H, Gu J, Li W, et al. (2020) Analysis of compressibility and mechanical behavior of red clay considering structural strength. *Arab J Geosci* 13: 411. https://doi.org/10.1007/s12517-020-05352-4
4. Zhang Y, Yang G, Chen W, et al. (2022) Relation between microstructures and macroscopic mechanical properties of earthen-site soils. *Materials* 15: 6124. https://doi.org/10.3390/ma15176124
5. Hu Q, Song W, Hu J (2023) Study of the mechanical properties and water stability of microbially cured, coir-fiber-reinforced clay soil. *Sustainability* 15: 13261. https://doi.org/10.3390/su151713261
6. Ge S, Zang J, Wang Y, et al. (2021) Combined stabilization/solidification and electroosmosis treatments for dredged marine silt. *Mar Georesour Geotechnol* 39: 1157–1166. https://doi.org/10.1080/1064119X.2020.1817205
7. Bahadori H, Hasheminezhad A, Taghizadeh F (2019) Experimental study on marl soil stabilization using natural pozzolans. *J Mater Civ Eng* 31: 04018363. https://doi.org/10.1061/(ASCE)MT.1943-5533.0002577
8. Peethamparan S, Olek J, Diamond S (2009) Mechanism of stabilization of Na-montmorillonite clay with cement kiln dust. *Cem Concr Res* 39: 580–589. https://doi.org/10.1016/j.cemconres.2009.03.013
9. Bahadori H, Hasheminezhad A, Mohamadi Asl S (2022) Stabilisation of urmia lake peat using natural and artificial pozzolans. *Proc Inst Civ Eng Ground Improv* 175: 104–113. https://doi.org/10.1680/jgrim.19.00024
10. Song Y, Geng Y, Dong S, et al. (2023) Study on mechanical properties and microstructure of basalt fiber-modified red clay. *Sustainability* 15: 4411. https://doi.org/10.3390/su15054411
11. Petry TM, Little DN (2002) Review of stabilization of clays and expansive soils in pavements and lightly loaded structures-history, practice, and future. *J Mater Civ Eng* 14: 447–460. https://doi.org/10.1061/(ASCE)0899-1561(2002)14:6(447)
12. Medvey B, Dobszay G (2020) Durability of stabilized earthen constructions: A review. *Geotech Geol Eng* 38: 2403–2425. https://doi.org/10.1007/s10706-020-01208-6
13. Anburuvel A (2023) The engineering behind soil stabilization with additives: a state-of-the-art review. *Geotech Geol Eng* 42: 1–42. https://doi.org/10.1007/s10706-023-02554-x

14. Lemaire K, Deneele D, Bonnet S, et al. (2013) Effects of lime and cement treatment on the physiochemical, microstructural and mechanical characteristics of a plastic silt. *Eng Geol* 166: 255–261. http://dx.doi.org/10.1016/j.enggeo.2013.09.012
15. Miraki H, Shariatmadari N, Ghadir P, et al. (2022) Clayey soil stabilization using alkali-activated volcanic ash and slag. *J Rock Mech Geotech Eng* 14: 576–591. https://doi.org/10.1016/j.jrmge.2021.08.012
16. Fonseca A, Cruz R, Consoli N (2009) Strength properties of sandy soil-cement admixtures. *Geotech Geol Eng* 27: 681–686. http://dx.doi.org/10.1007/s10706-009-9267-y
17. Mitchell, J, El Jack S (1966) The fabric of soil-cement and its formation. *Clays Clay Miner* 14: 297–305. https://doi.org/10.1346/CCMN.1966.0140126
18. Islam M, Hashim R (2009) Bearing capacity of stabilized tropical peat by deep mixing method. *Aust J Basic Appl Sci* 3: 682–688. http://www.ajbasweb.com/old/ajbas/2009/682-688
19. Horpibulsuk S, Rachan R, Suddeepong A (2011) Assessment of strength development in blended cement admixed bangkok clay. *Constr Build Mater* 25: 1521–1531. https://doi.org/10.1016/j.conbuildmat.2010.08.006
20. Du C, Zhang J, Yang G, et al. (2021) The influence of organic matter on the strength development of cement-stabilized marine soft clay. *Mar Georesour Geotech* 39: 983–993. https://doi.org/10.1080/1064119X.2020.1792593
21. Horpibulsuk S, Miura N, Bergado DT (2004) Undrained shear behavior of cement admixed clay at high water content. *J Geotech Geoenviron Eng ASCE* 130: 1096–1105. https://doi.org/10.1061/(ASCE)1090-0241(2004)130:10(1096)
22. Horpibulsuk S, Miura N (2001) A new approach for studying behavior of cement stabilized clays. Proceedings of the 15th international conference on soil mechanics and geotechnical engineering (ISSMGE), Istanbul, Turkey, 1759–1762. Available from: https://www.issmge.org/publications/online-library.
23. Miura N, Horpibulsuk S, Nagaraj TS (2001) Engineering behavior of cement stabilized clay at high water content. *Soils Found* 41: 33–45. https://doi.org/10.3208/sandf.41.5_33
24. Horpibulsuk S, Miura N, Nagaraj TS (2005) Clay-water/cement ratio identity of cement admixed soft clay. *J Geotech Geoenviron Eng ASCE* 131: 187–192. https://doi.org/10.1061/(ASCE)1090-0241(2005)131:2(187)
25. Zhou L, Shen X, Bai Z, et al. (2009) Experimental study on the effect of external admixtures on the modification of cemented soils. *Ind Constr* 39: 74–78 (in Chinese). https://doi.org/10.13204/j.gyjz2009.07.022
26. Wang J, Ding G, Pan L, et al. (2010) Study on mechanical properties and constitutive modeling of cemented soils in static triaxial tests. *Rock Soil Mech* 31: 1407–1412 (in Chinese). https://doi.org/10.16285/j.rsm2010.05.043
27. Shihata S, Baghdadi Z (2001) Simplified method to assess freeze-thaw durability of soil cement. *J Mater Civ Eng* 13: 243–247. https://doi.org/10.1061/(ASCE)0899-1561(2001)13:4(243)
28. Bouassida M, Porbaha A (2004) Ultimate bearing capacity of soft clays reinforced by a group of columns-application to a deep mixing technique. *Soils Found* 44: 91–101. https://doi.org/10.3208/sandf.44.3_91
29. Horpibulsuk S, Liu D, Liyanapathirana S, et al. (2010) Behaviour of cemented clay simulated via the theoretical framework of the structured cam clay model. *Comput Geotech* 37: 1–9. https://doi.org/10.1016/j.compgeo.2009.06.007

30. Jongpradist P, Youwai S, Jaturapitakkul C (2010) Effective void ratio for assessing the mechanical properties of cement-clay admixtures at high water content. *J Geotech Geoenviron Eng* 137: 621–627. https://doi.org/10.1061/(ASCE)GT.1943-5606.0000462
31. Wang H, Shen X, Wang X, et al. (2012) Experimental study on mechanical properties and microstructure of cement mortar composite soil. *Chin J Rock Mech Eng* 31: 3264–3269 (in Chinese).
32. Farouk A, Shahien M (2013) Ground improvement using soil-cement columns: Experimental investigation. *Alex Eng J* 52: 733–740. http://dx.doi.org/10.1016/j.aej.2013.08.009
33. Gyeongo K, Takashi T, Athapaththu A (2013) Strength mobilization of cement-treated dredged clay during the early stages of curing. *Soils Found* 2: 375–392. http://dx.doi.org/10.1016/j.sandf.2015.02.012
34. Chian S, Chim Y, Wong J (2016) Influence of sand impurities in cement-treated clays. *Géotechnique* 67: 31–41. https://doi.org/10.1680/jgeot.15.P.179
35. Du J, Liu B, Wang Z, et al. (2021) Dynamic behavior of cement-stabilized organic-matter disseminated sand under cyclic triaxial condition. *Soil Dyn Earthq Eng* 147: 106777. https://doi.org/10.1016/j.soildyn.2021.106777
36. Wahab N, Talib M, Malik A, et al. (2023) Effect of cement stabilized peat on strength, microstructure, and chemical analysis. *Phys Chem Earth Parts A/B/C* 129: 103348. https://doi.org/10.1016/j.pce.2022.103348
37. Fatahi B, Le T, Fatahi B, et al. (2013) Shrinkage properties of soft clay treated with cement and geofibers. *Geotech Geol Eng* 31: 1421–1435. https://doi.org/10.1007s/10706-013-9666-y
38. Du Y, Jiang N, Liu S, et al. (2014) Engineering properties and microstructural characteristics of cement-stabilized zinc-contaminated kaolin. *Can Geotech J* 51: 289–302. https://doi.org/10.1139/cgj-2013-0177
39. Zhao C, Zhao H, Chang Y, et al. (2014) Experimental study on physicochemical properties of cement-modified strongly expansive soils. *J Dalian Univ Technol* 6: 604–611 (in Chinese). https://doi.org/10.7511/dllgxb201406002
40. Liang S, Zeng W (2018) Experimental study of nansha silt soil reinforced with cement and fly-ash during wetting-drying cycles. *Ind Constr* 48: 83–86 (in Chinese). https://doi.org/10.13204/j.gyjz201807015
41. Zidan A (2020) Strength and consolidation characteristics for cement stabilized cohesive soil considering consistency index. *Geotech Geol Eng* 38: 5341–5353. https://doi.org/10.1007/s10706-020-01367-6
42. Phutthananon C, Jongpradist P, Nakin S, et al. (2022) State parameter governing the mechanical properties of cement-treated clays. *Mar Georesources Geotechnol* 41: 388–399. https://doi.org/10.1080/1064119X.2022.2049935
43. Sai Chandu A, Rama Subba Rao GV (2021) Strength and durability characteristics of red soil stabilised with foundry sand and cement. *Arab J Sci Eng* 46: 5171–5178. https://doi.org/10.1007/s13369-021-05423-y
44. Xu M, Liu L, Deng Y, et al. (2021) Influence of sand incorporation on unconfined compression strength of cement-based stabilized soft clay. *Soils Found* 61: 1132–1141. https://doi.org/10.1016/j.sandf.2021.06.008

45. Liang S, Wang Y, Feng D (2023) Experimental study on strength and dry-wet cycle characteristics of south China coastal soft soil solidified by cement collaborating sand particles. *Appl Sci* 13: 8844. https://doi.org/10.3390/app13158844
46. Nakayenga J, Mutsuko I, Guharay A, et al. (2023) Effect of limestone and granite stone powder on properties of cement-treated clay composites and their socioeconomic and environmental impacts. *Constr Build Mater* 393: 132064. https://doi.org/10.1016/j.conbuildmat.2023.132064
47. Phutthananon C, Tiyawan N, Jongpradist P, et al. (2023) Investigation of strength and microstructural characteristics of blended cement-admixed clay with bottom ash. *Sustainability* 15: 3795. https://doi.org/10.3390/su15043795
48. Chen C, Zhang C, Liu X, et al. (2023) Effects of freeze-thaw cycles on permeability behavior and desiccation cracking of dalian red clay in China considering saline intrusion. *Sustainability* 15: 3858. https://doi.org/10.3390/su15043858
49. Yarba N, Kalkan E, Akbulut S (2007) Modification of the geotechnical properties, as influenced by freeze-thaw, of granular soils with waste additives. *Cold Reg Sci Technol* 48: 44–54. https://doi.org/10.1016/j.coldregions.2006.09.009
50. Liu J, Wang T, Tian Y (2010) Experimental study of the dynamic properties of cement- and lime-modified clay soils subjected to freeze–thaw cycles. *Cold Reg Sci Technol* 61: 29–33. https://doi.org/10.1016/j.coldregions.2010.01.002
51. Sagidullina N, Abdialim S, Kim J, et al. (2022) Influence of freeze-thaw cycles on physical and mechanical properties of cement-treated silty sand. *Sustainability* 14: 7000. https://doi.org/10.3390/su14127000
52. Ma Z, Xing Z, Zhao Y, et al. (2023) Dynamic strength characteristics of cement-improved silty clay under the effect of freeze-thaw cycles. *Sustainability* 15: 3333. https://doi.org/10.3390/su15043333

AIMS Press